

INJECTOR DESIGN TOWARDS ERL-BASED EUV-FEL FOR LITHOGRAPHY

O. A. Tanaka[†], N. Nakamura, T. Miyajima, T. Tanikawa, High Energy Accelerator Research Organization (KEK), Tsukuba, Japan

Abstract

A high-power EUV light source using ERL-based FEL can supply multiple semiconductor exposure devices. There are some requirements in the whole and its injector, in particular, and their examination and necessary development are being carried out. The requirement for the injector was to generate high bunch charge beams at a high-repetition rate. In this regard, a space charge effect should be treated carefully in the design of the injector. For FEL operation, not only short bunch length and small transverse emittance but also small longitudinal emittance are required. By using a multi-objective genetic algorithm, we are minimizing them at the exit of the injector to investigate the injector performance and its effect on the FEL generation. In this study, we describe the injector optimization strategies and possible options suited for the ERL-based EUV-FEL.

INTRODUCTION

An energy-recovery linac (ERL) based free-electron laser (FEL) as an extreme ultraviolet (EUV) light source has been designed using available technologies to demonstrate a generation of EUV power of more than 10 kW that supplies multiple semiconductor exposure devices [1, 2]. Figure 1 shows the schematic of the EUV light source using ERL-based FEL [1]. An electron beam is accelerated to 10.5 MeV at an exit of the injector section, and then to 800 MeV at an exit of the main linac. A final bunch compression is done using the 1st arc section to obtain a high peak current which will be required for SASE-FEL generation. After the bunch compression, the electron beam is sent to an undulator section to produce 13.5 nm EUV-FEL light. After the FEL generation the bunch is delivered to the 2nd arc section, and it will be decelerated by the main linac as energy recovery, and then disposed into a beam dump.

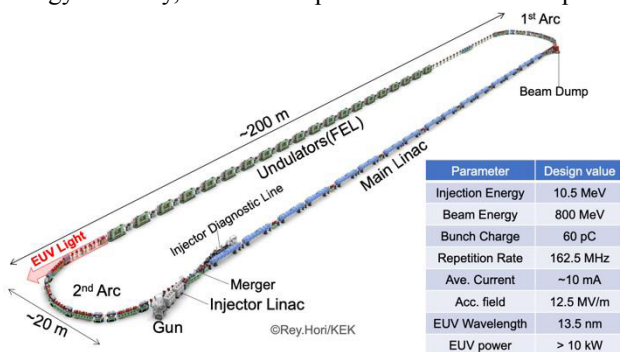


Figure 1: Design and specification of the ERL-based EUV-FEL light source for lithography.

[†] olga@post.kek.jp

With a bunch charge of 60 pC and a bunch repetition frequency of 162.5 MHz, the average current of the electron beam is about 10 mA. The disposed beam power is reduced from 8 MW to 100 kW by the energy recovery process. Proof-of-concept of the EUV-FEL using the ERL test machine at KEK (cERL) is given in Ref. [3, 4].

The goal of the injector design for the EUV-FEL is to deliver the beam with the proper quality at the injector exit [5]. The “proper beam quality” includes:

1. Bunch length is less than 3 ps;
2. Transverse emittance is less than 3π mm mrad;
3. Longitudinal emittance is less than 10 keV ps.

In the previous work the injector has been optimized by a specific target: minimizing both the bunch length and the transverse emittance. This strategy gave an unreasonably large value of the longitudinal emittance (7.25 keV ps), while the transverse emittance was kept small enough (0.63 π mm mrad) at the injector exit. That resulted in the charge density relaxation at the FEL, and, consequently, in deficient FEL power.

In order to improve the beam quality, we have changed the designing strategy for the injector to minimize not only 1. and 2., but also 3. The discussion on how the new strategy affected the beam quality is given in the following.

In the present work we will give a comparison of ‘old’ and ‘new’ injector designs.

OPTIMIZATION METHOD

To clarify the optimization method used in this work, let us first introduce the layout of the EUV-FEL injector. As shown in Fig. 2, it consists of 3 sections: the injector section, the matching section, and the merger section. The injector section includes a 500 kV cERL-type DC electron gun to produce a stable electron beam, 2 solenoids to control the transverse beam size, a buncher cavity placed between 2 solenoids to compress the bunch length, and 2 superconducting cryomodules with 3 2-cell cavities each. Then the electron beam is reached to 10.5 MeV. The matching section includes 4 quadrupoles to match the injector optics to that of the recirculation loop. At last, the merger section consists of 3 bending magnets to guide the beam trajectory to the recirculation loop and 2 quadrupoles to facilitate the optics matching [6]. The matching point

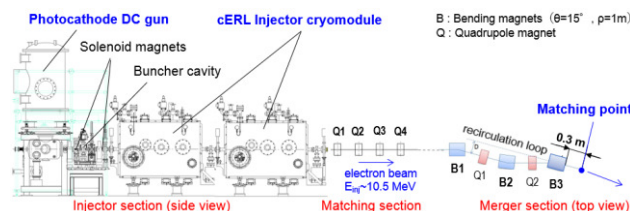


Figure 2: Schematic of the EUV-FEL injector.

(located 0.3 m downstream of the edge of B3 in Fig.2) is chosen just after the merger section, since it makes the space charge control in the injector easier. The main parameters for the injector are listed in Table 1. Other parameters such as initial laser spot diameter, laser pulse length, buncher voltage etc. are defined by the injector optimization results. They are discussed later.

Table 1: Main Parameters in the EUV-FEL Injector

Electron gun voltage	500 kV
Bunch charge	60 pC
Injector beam energy	10.5 MeV
RF frequency	1.3 GHz
Cavities' acceleration field	< 7.3 MV/m

The maximum electron energy in this simulation is 10.5 MeV, and the space charge effect cannot be ignored. Therefore, we used the particle tracking code GPT (General Particle Tracer) [7] including the effect. We have studied the transport conditions that are compatible with small longitudinal emittance and short bunch length. The set of parameters that realizes such transportation includes 26 variables listed in Table 2. Detailed information on variables and objectives in the previous study can be found in Ref. [6].

The Multi-Objective Genetic Algorithm (MOGA) [8] is used as the optimization method. The target of the algorithm is the simultaneous minimization of the bunch length and the transverse emittance ('old' strategy); the bunch length and the longitudinal emittance with additional constraint applied to the transverse emittance (< 3 π mm mrad, 'new' strategy); at the matching point (see Fig. 2). In order to minimize the parameters, the GPT tracking is first performed under appropriate starting conditions. Then the transport conditions are gradually changed according to the genetic algorithm to meet the optimization target. If enough trials are repeated, the curves shown in Fig. 3 will be obtained for the two parameters to be optimized: the bunch length and the longitudinal (transverse) emittance. The bunch charge is 60 pC and the number of macro particles is 500 k.

OPTIMIZATION RESULTS

The comparison of the results obtained using 'old' and 'new' strategies is given in Fig. 3. Thus, the top plot represents optimized longitudinal emittance and energy spread as a function of the bunch length at the exit of the merger. Apparently, the 'new' approach yielded clear and beautiful Pareto front with fewer values of the longitudinal emittances, since those minimizations were the original target of the optimization. It is opposite for the bottom plot, where the optimized transverse emittances are shown as a function of the bunch length at the exit of the merger.

Once the transportation variables listed in Table 2 are derived, the beam performance at the injector exit can be studied by calculating the envelope and particle distributions with the bunch length fixed. To be concrete, it is fixed to 1 ps in the following discussion. The results of the dedicated tracking with 500 k macro particles were done for both 'old' and 'new' designs (see Fig.4). The top plot

Table 2: Variables

Laser spot diameter	1.21 mm
Laser pulse length ¹	13.75 ps
SL1 solenoid current	4.42 A
SL2 solenoid current	1.57 A
Buncher cavity. voltage	91.94 kV
Buncher cavity phase offset	-90.99 deg.
Inj1 cavity voltage	6.80 MV/m
Inj2 cavity voltage	7.99 MV/m
Inj3 cavity voltage	7.99 MV/m
Inj4 cavity voltage	7.99 MV/m
Inj5 cavity voltage	7.99 MV/m
Inj6 cavity voltage	7.99 MV/m
Inj1 cavity phase offset	-33.82 deg.
Inj2 cavity phase offset	-27.44 deg.
Inj3 cavity phase offset	-19.00 deg.
Inj4 cavity phase offset	3.73 deg.
Inj5 cavity phase offset	18.46 deg.
Inj6 cavity phase offset	0.59 deg.
Distances between:	
gun and solenoid 1	0.30 m
solenoid 1 and buncher	0.37 m
buncher and solenoid 2	0.13 m
solenoid 2 and cavity 1	1.38 m
Q1 quadrupole straight	16.23 / m ²
Q2 quadrupole straight	-13.72 / m ²
Q3 quadrupole straight	-4.12 / m ²
Q4 quadrupole straight	8.94 / m ²

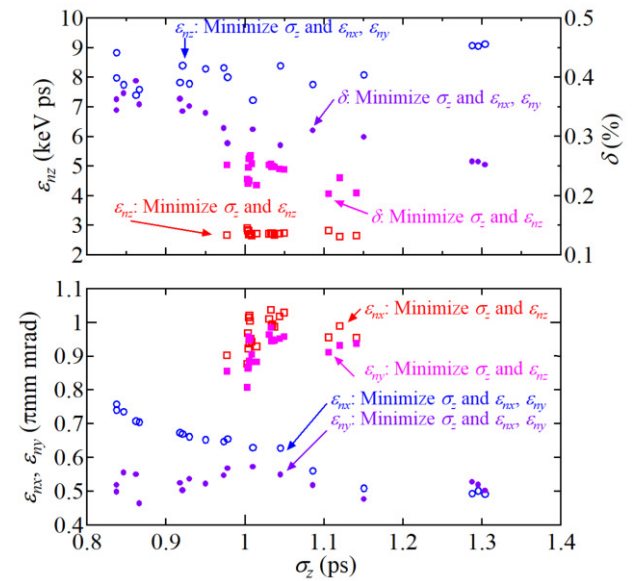


Figure 3: Optimized longitudinal emittance and energy spread (top) and transverse emittance (bottom) as a function of the bunch length at the exit of the merger.

¹ full width of the uniform distribution.

shows the time evolution of longitudinal emittances through the injector, the middle does energy spreads, and the bottom does transverse emittances. They are in full agreement with the results of optimizations given in Fig. 3. The final beam parameters obtained through the envelope calculation are summarized in Table 3. At the fixed bunch lengths one can see more than 2.7 times decrease in the longitudinal emittance and 1.4 times decrease in the energy spread within the ‘new’ strategy of optimization. The transverse emittance increased by about 1.5 times compared with the ‘old’ design.

A smaller beam transverse emittance, which is proportional to the square of the beam transverse size, is associated with a higher FEL gain. Also in practice, the lower limit for the transverse emittance is set at the injector exit, beyond which the transverse space charge forces become quite small and no longer act to rearrange the particles in phase space [9]. The normalized longitudinal emittance scales as the product of bunch length and energy spread [10]. Therefore, for a fixed bunch length, a smaller value of the energy spread is considered more favorable for the production of FEL, since the amplification rate of the FEL signal (gain) increases as the energy spread of electrons

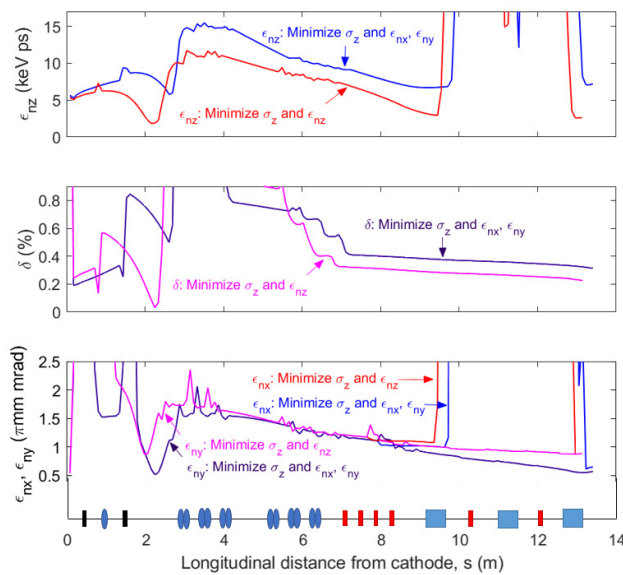


Figure 4: Tracking results of the optimized longitudinal emittances (top); energy spreads (middle); transverse emittances (bottom) through the injector.

Table 3: Beam Parameters at the Injector Exit

	‘Old’	‘New’
Bunch length σ_z [ps]	1.00	1.00
Long. emittance ϵ_{nz} [keV ps]	7.25	2.66
Hor. emittance ϵ_{nx} [π mm mrad]	0.63	0.94
Vert. emittance ϵ_{ny} [π mm mrad]	0.58	0.88
Hor. Beam size σ_x [mm]	0.81	0.99
Vert. beam size, σ_y [mm]	1.52	1.49
Energy spread δ [%]	0.31	0.22

decreases [11]. An ultimate examination of the results of these two injector optimization strategies should be done downstream in the recirculation loop. This examination includes bunch compression at the arc section and FEL generation in the undulator section. These studies are out of the scope of the present work.

Now let’s consider particle distribution comparison at the injector exit. 500 k particles distributions have been tracked. Phase spaces and temporal histograms have been compared in Fig. 5. The left side figures show the ‘old’ design, and those of the right side show the ‘new’ one. Apparently, the phase space (Fig. 5 (b)) has been linearized compared with the previous study (Fig. 5 (a)). The longitudinal emittance has been intentionally minimized. That has made the energy spread smaller. As for temporal histograms, the current result (Fig. 5 (d)) demonstrates less particle density spike in the left part of the histogram compared with the previous one (Fig. 5 (c)). The spike doesn’t affect the FEL gain essentially because the longitudinal space charge effect considerably relaxes the spike in the main linac acceleration.

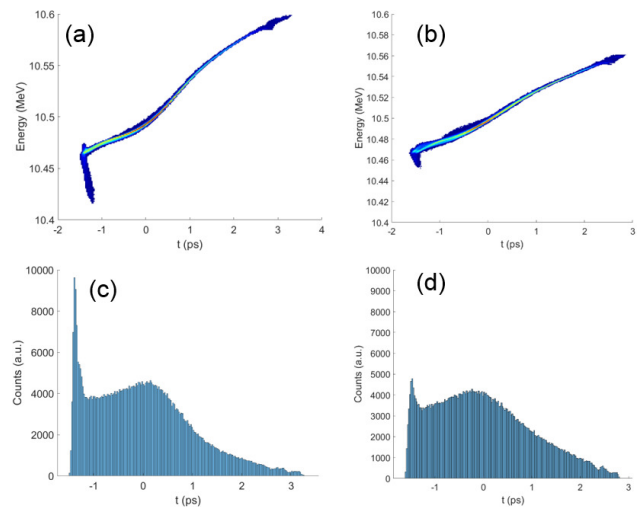


Figure 5: Particle distribution comparison: the phase space (a) and the temporal histogram (c) in the ‘old’ design; (b) and (d) are those for the ‘new’ design.

CONCLUSION

In the present injector study, we improved the beam quality at the injector exit, by changing the optimization strategy to the simultaneous minimization of the bunch length and the longitudinal emittance with additional constraints applied to the transverse emittance. This improvement allows a better beam quality at the matching point, namely: more than 2.7 times decrease in the longitudinal emittance and 1.5 times decrease in the energy spread. Although the maximum values of the transverse emittance are increased by 1.5 times compared with the ‘old’ design. The discussion on the reasonableness of the current improvement will be continued after its proper examination in the recirculation loop (i.e. in the arc and undulator sections).

REFERENCES

- [1] N. Nakamura, “EUV ERLs for Semiconductor Integrated Circuits Lithography”, in *Proc. of ERL2017*, CERN, Geneva, Switzerland, Jun. 2017, paper TUIBCC002.
https://accel-conf.web.cern.ch/erl2017/talks/tuibcc002_talk.pdf
- [2] N. Nakamura *et al.*, “Design Work of the ERL-FEL as the High Intense EUV Light Source”, in *Proc. of ERL2015*, Stony Brook, NY, USA, Jun. 2015, pp. 4-9,
<http://jacow.org/ERL2015/papers/mopcth010.pdf>
- [3] H. Kawata *et al.*, “High Repetition Rate (81.25MHz) FEL Project Based on cERL”, in *Proc. of 2019 EUVL Workshop*, Berkley, CA, USA, Jun. 2019, paper P045.
<https://www.euvlitho.com/2019/P45.pdf>
- [4] R. Kato *et al.*, “Stepwise Development to Realize the High Power EUV-FEL Light Source” in *Proc. of OSA High-brightness Sources and Light-driven Interactions Congress 2020 (EUVXRAY, HILAS, MICS)*, Washington, DC, USA, Nov. 2020, paper ETh2A.2.
<https://doi.org/10.1364/EUVXRAY.2020.ETH2A.2>
- [5] R. Kato, private communications, Jan. 2022.
- [6] T. Hotei and T. Miyajima, “Optics matching of EUV-FEL injector”, in *Proc. PASJ2016*, Chiba, Japan, Aug. 2016, pp. 1049-1052.
https://www.pasj.jp/web_public/pasj2016/proceedings/PDF/TUP0/TUP069.pdf
- [7] Pulsar Physics,
<http://www.pulsar.nl/gpt/index.html>
- [8] C. M. Fonseca and P. J. Fleming, “Genetic Algorithms for Multiobjective Optimization: Formulation Discussion and Generalization”, in *Proceedings of the 5th International Conference on Genetic Algorithms*, San Francisco, CA, USA, Jun. 1993.
ISBN: 978-1-55860-299-1
- [9] C. Leujeune and J. Aubert, *Emitance and Brightness: Definitions and Measurements*. Academic Press, Inc.: Paris, France, 1980.
- [10] S. Di Mitri, “Novel techniques for future TeV electron accelerators”, in *Proc. IPAC’18*, Vancouver, BC, Canada, Apr.-May 2018, pp. 57-59.
doi:10.18429/JACoW-IPAC2018-PAPERID
- [11] S. Di Mitri, “On the Importance of Electron Beam Brightness in High Gain Free Electron Lasers”, *Photonics*, vol. 2, no. 2, Mar. 2015, pp. 317-341.
doi:10.3390/photonics2020317